Int J Clin Exp Pathol 2021;14(5):582-595
www.ijcep.com /ISSN:1936-2625/IJCEP0121428

Original Article

Integrative analysis of somatic mutations and differential expression profiles in glioblastoma based on aging acceleration

Huize Wang[1,2], Shiyan Li[3], Hongxin Liu[3], Shiyu Bian[4], Wanjiang Huang[5], Chengzhong Xing[2], Yin Wang[2,3]

[1]Department of Nursing, First Affiliated Hospital of China Medical University, 155# North Nanjing Street, Shenyang 110001, Liaoning, China; [2]Tumor Etiology and Screening Department of Cancer Institute and General Surgery, The First Affiliated Hospital of China Medical University, 155# North Nanjing Street, Heping District, Shenyang 110001, Liaoning Province, China; [3]Department of Biomedical Engineering, School of Fundamental Sciences, China Medical University, Shenyang 110122, Liaoning Province, China; [4]China Medical University - The Queen's University of Belfast Joint College, China Medical University, Shenyang 110122, Liaoning Province, China; [5]No. 10 Middle School, Xiangyang 441021, Hubei Province, China

Received August 31, 2020; Accepted February 7, 2021; Epub May 15, 2021; Published May 30, 2021

Abstract: Background: Glioblastoma (GBM) is an aggressive brain tumor and the mechanisms of progression are very complex. Accelerated aging is a driving factor of GBM. However, there has not been thorough research about the mechanisms of GBM progression based on aging acceleration. Methods: The aging predictor was modeled based on normal brain samples. Then an aging acceleration background network was constructed to explore GBM mechanisms. Results: The accelerated aging-related mechanisms provided an innovative way to study GBM, wherein integrative analysis of somatic mutations and differential expression revealed key pathologic characteristics. Moreover, the influence of the immune system, the nervous system and other critical factors on GBM were identified. The survival analysis also disclosed crucial GBM markers. Conclusion: An integrative analysis of multi-omics data based on aging acceleration identified new driving factors for GBM.

Keywords: Aging, glioblastoma, integrative analysis, network analysis

Introduction

Much research has indicated that there are relationships between cancers and aging; further, it also has been held that cancers cannot be isolated from the effects of accumulated genetic mutations without accelerated aging [1, 2]. Fortunately, integrating genomics and transcriptomics has been deeply rooted in the public mind [3]. Therefore, exploring the mechanisms between aging and traditional cancer markers (i.e. mutations and differential expression) is a powerful approach to study the progression of GBM.

Actually, cancers may be promoted by a decline in cellular functions, (i.e. a dysregulated immune system), often induced by accelerated aging, which has been identified as an intrinsic risk factor for cancers [3]. According to statistics, the majority of cancer victims are elderly. This highlighted the necessity for the clinical practice of geriatric oncology.

Among past achievements, a series of GBM markers has been identified (i.e. through differential expression) [4]. Fortunately, The Cancer Genome Atlas (TCGA) database generated a large amount of required cancer data, including somatic mutations, gene expression, and clinical follow-up profiles; the GEO platform also provided relative profiles (i.e. healthy persons). However, an integrative analysis of GBM based on aging acceleration has not been studied thoroughly.

In this manuscript, a series of works were represented by the following flow chart (**Figure 1**): (1) modelling the aging predictor; (2) exploring crucial accelerated aging-related somatic muta-

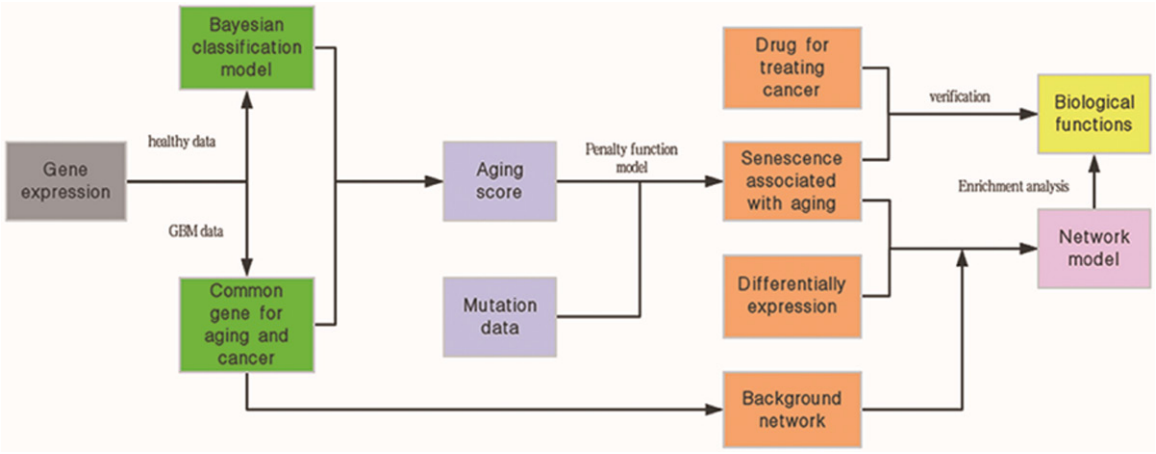

Figure 1. The computational flow chart.

tions based on aging acceleration; (3) integrating the accelerated aging-related mutations and differential expression based on the aging acceleration background network; (4) investigating the biologic functions of the "accelerated aging-related SNPs to differential expression" modules. In short, the mechanisms of GBM progression associated with aging acceleration were explored in this paper.

Materials and methods

Modelling the aging predictor using normal brain data

We obtained the transcriptional profiles of healthy persons (584 samples) from the Gene Expression Omnibus (GEO) platform (GSE15-745). The brain tissues included the cerebellum, frontal cortex, pons, and temporal cortex. We then divided all samples into two groups (old age samples ≥50 and young samples < 50). Then about two-thirds of the samples were randomly selected as the training subsets and the remaining proportion were set as the test subsets for each age group, respectively. Ultimately, the training subsets in the young and old groups were combined into the total training set, as well as the total test set.

The feature selection pipeline of the aging predictor was performed as follows:

(1) The weight of each feature was calculated in the training sets with the help of the ReliefF algorithm. For classification, the ReliefF used K nearest neighbors per class, ranking indices of columns ordered by attribute importance, with large positive weights assigned to important attributes. In this work, the value of K was set to 10.

(2) According to the law of decreasing importance of the characteristics, the test set features were also sorted based on the training data.

(3) The prediction result of the age group was calculated using the Naive Bayesian classifier, assigning each sample to the most probable class (using the maximum a posteriori decision rule):

$$P(Y = k \mid X) = \frac{\pi(Y = k)\prod_{j=1}^{p} P(X_j \mid Y = k)}{\sum_{k=1}^{K} \pi(Y = k)\prod_{j=1}^{p} P(X_j \mid Y = k)} \quad (1)$$

Where X was each sample, Y was the phenotype (the class of each class, i.e. the young or old age group in this work), and $\pi(Y=k)$ was the prior probability of each class (set as 0.5 in this work).

(4) To pick out the optimal model predictor which contained the maximum average correct rate, we adopted the five-fold cross-validation for the total training set; then taking advantage of the selected model, we computed the accuracy in the total test set. Consequently, both the learning curve and the ROC curve were summarized.

Accelerated aging patterns in GBM

We downloaded cancer genome data from the TCGA and GEO (GSE15745) database, and standardized 11,378 cancer genes' (the genes shared by both normal tissue and cancerous tissue were selected) expression levels. As a comparison with healthy tissue, the best model was selected as mentioned in the normal samples. Then in line with prediction outcomes, a posteriori probabilities (in the Bayesian classifier) were treated as aging scores. The median aging scores were defined as an overall grade for the certain age groups (≥50 years old, ≥60 years old, ≥70 years old and ≥80 years old) and the differences between GBM patients and the healthy group were revealed. The Kruskal Wallis test was used to test the difference between the healthy people and GBM patients, and significance was set at *p*-value < 0.05.

Identifying accelerated aging related somatic mutations

Since the mutation and the transcriptional profiles contain different genes, we extracted the identical genes shared by both mutation and the expression profiles, and then selected relevant mutation data. To pick out the SNP set with the best fitting result, the elastic net algorithm was used. The five-fold cross-validation was performed, which calculated a least-squares regression coefficients for a set of regularization coefficients:

$$B = \arg\min\left(\frac{1}{2N}\sum (Y - X * B)^2 + \frac{\lambda}{2}\left(\| B \|^2 + \| B \|\right)\right) \quad (2)$$

Where B was the regression coefficient, N was the number of training data, and λ was the penalty term (determined by the 5-fold cross validation in this work).

In order to select the optimal model in the five-fold cross-validation progress, the minimum average of the mean squared error (MSE) was used as the standard. As a result, the elastic net method was used on the total data to determine the number of selected mutations, if the coefficient was not 0.

Constructing the aging acceleration background network

Both the Pearson correlation coefficient and the partial correlation coefficient (based on the aging score) between each pair of genes were calculated. Whenever correlation and partial correlation coefficients had opposite signs, the relevant two genes might be related to aging acceleration. Then the criterion of $P < 0.05$ and the False Discovery Rate (FDR) < 0.2 in either correlation or partial correlation coefficient was used to determine each pair of genes to form the edge of the background network. As a result, each module of "accelerated aging related mutation to differential expression" was identified by exploring the shortest path in the aging acceleration network using the Dijkstra algorithm.

Enrichment analysis

To find vital biological significance, enrichment analysis was put to use, using Gene Ontology terms and KEGG pathways, both of which stem from Gene Set Enrichment Analysis (GSEA) platform (http://software.broadinstitute.org/gsea/downloads.jsp). We adopted the hypergeometric test to figure out significantly enriched KEGG pathways or Gene Ontology (GO) Biological Process (BP) terms. The hypergeometric distribution formula for test of the degree of enrichment about the selected gene sets is shown below.

$$P = 1 - \sum_{i=0}^{m-1} \frac{\binom{M}{i}\binom{N-M}{n-i}}{\binom{N}{n}} \quad (3)$$

Where N was the total number of genes in the gene list, M was the number of known gene sets (i.e. KEGG pathway, GO terms), n was the number of identified genes and i was the number of shared genes between known gene sets and identified genes. If $P < 0.05$ and FDR < 0.2, the selected GO terms or KEGG pathways were considered as a significantly enriched module.

Survival analysis

Whether the module had a significant effect on the patient's survival time or not still was worth of exploring. In order to study survival results, all patients were divided into a high expression group and low expression group based on the median of each gene expression. The Kaplan-Meier method was used to draw the survival curve and the log-rank test was used to check if there was a significant difference between the survival curves of the two groups, where $P < 0.05$ was used as the primary standard.

Table 1. The prediction results

	Old samples	Young samples	Accuracy
The training set	120	269	0.7632 (cross-validation)
The test set	60	135	0.7167

Results

The aging model revealed crucial GBM markers based on aging acceleration

The aging predictor was modeled based on transcriptional profiles using the Naive Bayesian classifier (**Table 1**). The five-fold cross-validation was applied to select the optimal model. As a result, it illustrated that the top 402 important markers were selected (accuracy =0.7167 in the test data). The learning curve and ROC curve (AUC=0.72098) are shown in **Figure 2**. The results proved that our model could predict the aging process with enough accuracy.

Further, to distinguish between the chronological age and aging acceleration, the aging scores were calculated using posterior probability of the Naive Bayesian classifier (**Table 2**). From the chart, the result shown that the aging scores indicated a growing trend with increasing ages; apart from this, the aging scores of the cancer samples were significantly higher than the scores of normal samples within different age groups, respectively. All involved *p*-values were lower than 0.05 using the Kruskal-Wallis test (**Figure 3A-D**). The details displayed in **Figure 3A-D** indicate aging acceleration in GBM.

To explore crucial genomic dysfunctions associated with accelerated aging, the relationships between somatic mutations and the aging acceleration pattern were identified using the elastic net. As a result, 24 somatic mutations were identified as key markers related to aging acceleration, whose frequencies are also summarized in **Table 3** and **Figure 4A**. For example, ABCB4 had the greatest absolute weight (0.2268) and TP53 had maximum frequency (0.2400). The functions of ABCB4 have been deeply investigated, and it plays an important role in the synthesis of phosphatidylcholine [5] as well as the restraining of anticancer drug resistance during cancer treatment [6]. It had a great association with immunity, affecting both cancer and aging. Besides, TP53 has been widely recognized as the crucial marker that inhibits cancer [7-9] by regulating the cell cycle, cell apoptosis, cell senescence, and the DNA damage repair [10]. In short, TP53 played an important role in on aging and cancer.

Critical functions were explored by integrating accelerated aging-related mutations and differential expression genes

To investigate GBM mechanism based on aging acceleration, herein the aging acceleration background network was constructed (totally containing 1948259 edges). Then the modules of "accelerated aging related SNP to differential expression" were identified based the aging acceleration background network. Further, an enrichment analysis was performed to explore biologic functions of these modules. As a result, 24 some key modules were enriched in biologic significance (Table S3 and Figure S1). These modules are shown in **Figure 4B** and **4C**, and the total gene lists were shown in Table S1.

For example, the most enriched KEGG pathway was interactions with endocytosis of cells (FDR=0.0612) driven by Clathrin. Clathrin was ubiquitously distributed [11], and CHC17 (representative of Clathrin) performs key functions in formation of the mitotic spindle that contribute to cancer cell proliferation and division [12].

Further, there were a series of "accelerated aging SNP to differential expression" enriched critical BP terms, indicating the dysfunction of the immune system and nervous system as well as the cellular homeostasis of GBM based on aging acceleration (**Figure 5**).

(1) The impact of the immune system on glioblastoma.

In the process of GO term analysis, the immunomodulatory-related terms were concentrated in the 12th and the 18th module. The results are displayed in **Figure 5A** and **Table 4**. Moreover, the gamma interferon regulates apoptosis and tumor suppressor pathway through immunological genes [13]. Thus in the reactive conditions, myeloid leukocytosis mediates immune response to regulate the diseases [14]. Leukocyte degranulation effect plays a role in cancer. Besides, the mast cell activation is effective to maintain survival [15]. Neutrophils (primarily white blood cells) are associated with immune function. Once neutrophil degranulation occurs, its phagocytic function is lost, influencing the

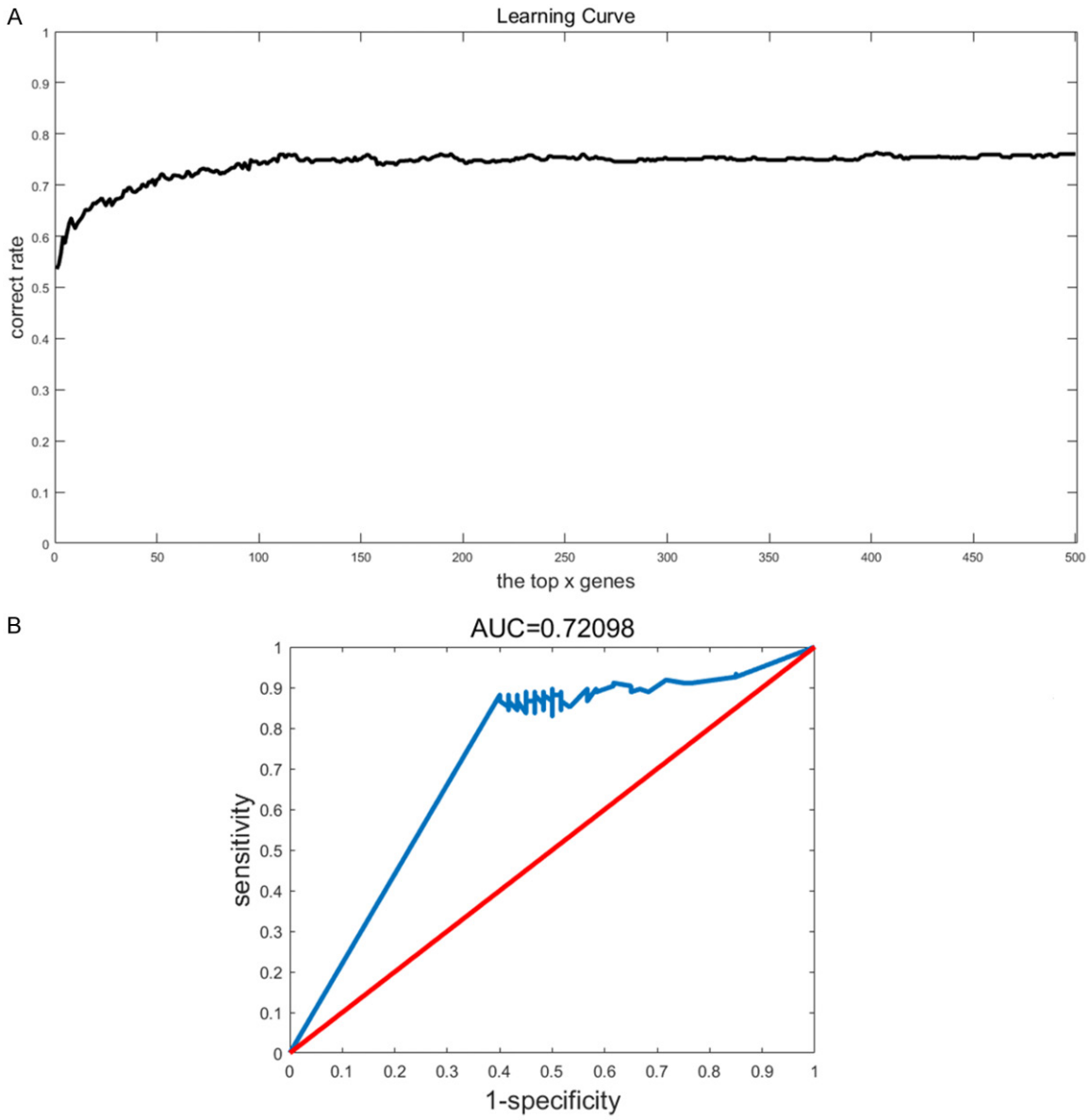

Figure 2. Results of the aging predictor. A. The learning curves by 5-fold cross-validation; B. The ROC curves.

Table 2. The median aging scores

In GBM	In normal brain	Age (years old)
7.4103e-13	1.0879e-26	≥50
5.1013e-12	2.1579e-24	≥60
5.804e-12	6.3590e-24	≥70
7.3753e-06	2.5671e-23	≥80

elimination of tumor factors [16]. Most members of the white blood cell family are involved in tumor suppression. Therefore, it was found that the enrichment results of GO terms revealed critical mechanisms of GBM.

(2) The nervous system-related reactions.

A total of 17 terms were enriched in the nerve cells and neuromodulation processes. Details are shown in **Table 5** and in **Figure 5B**. The neurological biological processes were enriched in the 12th, 18th and 19th module.

The top enriched modules indicated the dysfunction of glial cell production and differentiation. Malignancy of glioma increased with the degree of differentiation of tumor cells increasing [17]. That is, the division and differentiation of various nerve cells were mostly annotated in

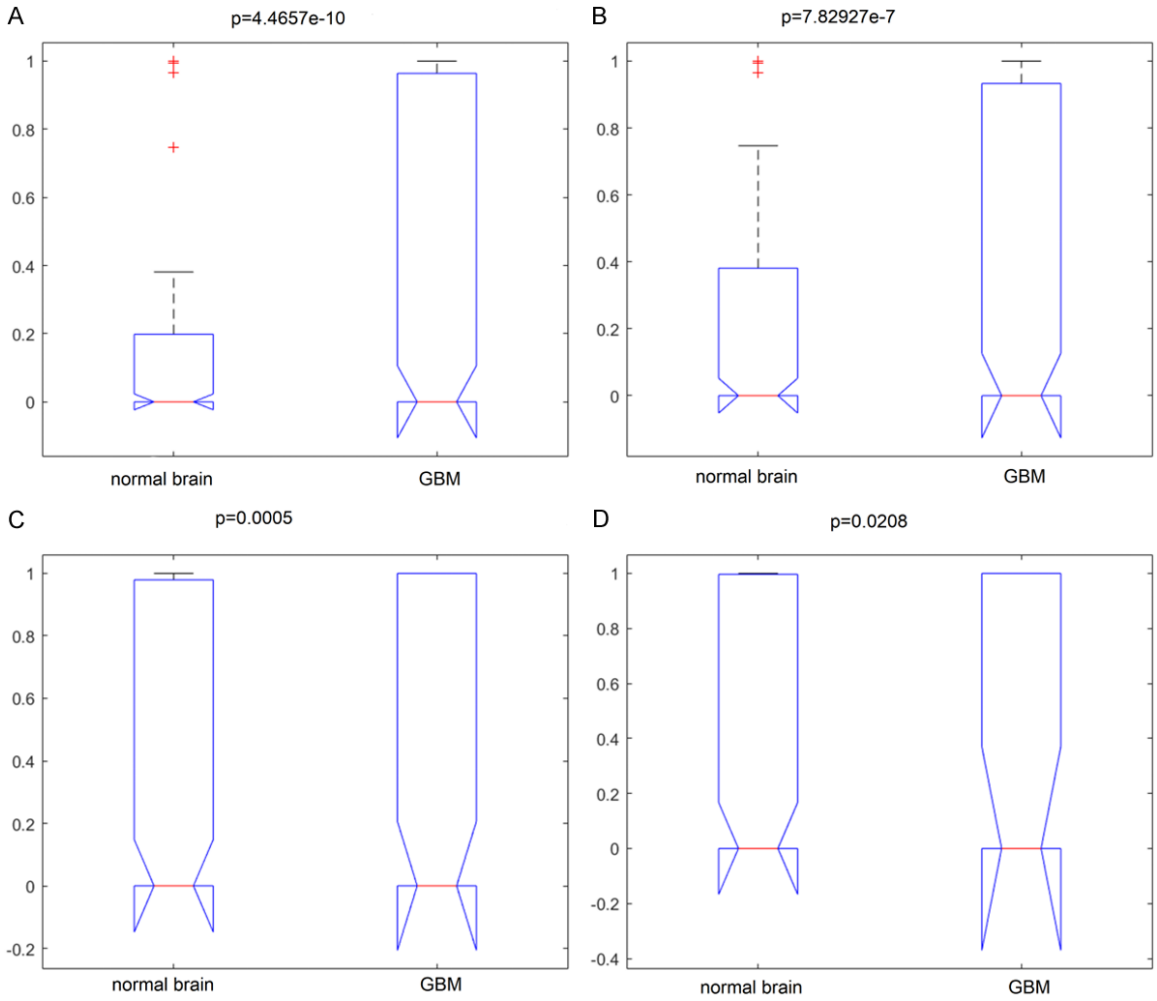

Figure 3. Aging acceleration results of GBM. A. 180 normal samples, 204 GBM samples (≥50 years old, p=4.4657e-10; B. 132 normal samples, 134 GBM samples (≥60 years old), P=7.82927e-07; C. 108 normal samples, 58 GBM samples (≥70 years old), P=0.005; D. 88 normal samples, 18 GBM samples (≥80 years old), P=0.0208.

Table 3. The mutations associated with aging

Gene symbol					
ITGA7	ITGAE	SLC38A1	USP16	ABCB4	AUTS2
PABPC3	DNAH17	SIGLEC8	KRT15	DMBT1	CEP76
CETP	DGKD	IKZF3	YY2	ZNF235	FGD6
CD7	AHNAK	PTPRM	ZBTB40	YIPF6	NEBL

terms of significant enrichment and affect the formation and spread of GBM [18]. Previous studies have shown that astrocytes and glial cells were prone to variability in an undifferentiated state [19]. Neuron projection extension was also enriched in the 12th module. The migration and connection of glioma cells cannot be separated from the extension of projections [20]. It could be inferred that the occurrence and deterioration of GBM were inseparable from the prolongation of neuronal processes. As well known, the movement activity of cells in the forebrain (including the telencephalon) plays an important role in maintaining the development of brain tissue, promoting the metastasis of brain tumors [21]. If the cell death were induced abnormally, the risk of cancer should increase [22]. The synapse is an important approach of neuron communication thus it has a significant impact on survival [23].

(3) Cells' response and changes to various stimulation and substances.

There were 12 terms enriched in the variation in cells stimulated by changeable substances, including oxygenates, nitrogenous compounds, hormones and so on. Related chart content

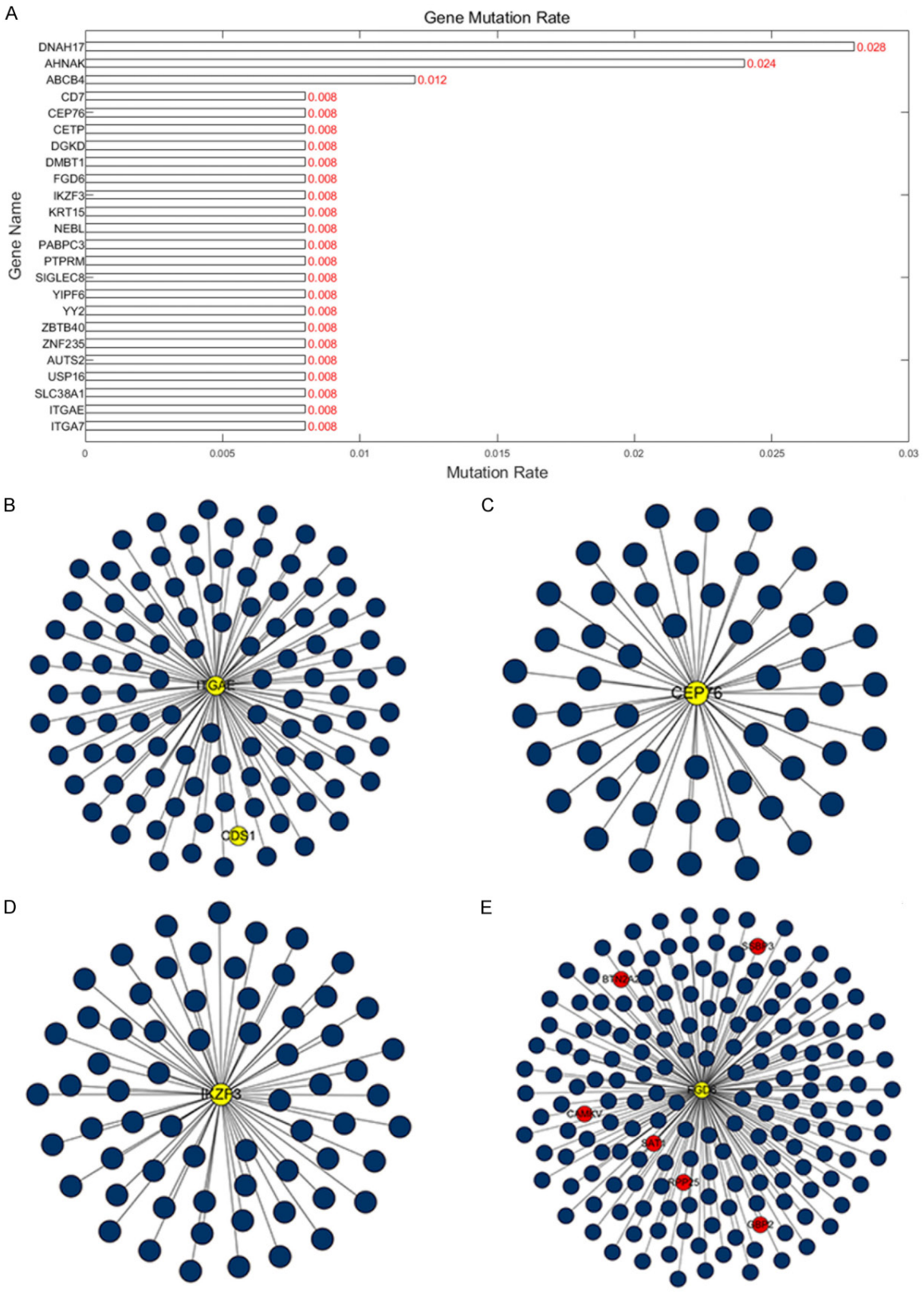
A
Gene Mutation Rate
DNAH17
AHNAK
ABCB4
CD7
CEP76
CETP
DGKD
DMBT1
FGD6
IKZF3
KRT15
NEBL
PABPC3
PTPRM
SIGLEC8
YIPF6
YY2
ZBTB40
ZNF235
AUTS2
USP16
SLC38A1
ITGAE
ITGA7
0.028
0.024
0.012
0.008
Gene Name
0
0.005
0.01
0.015
0.02
0.025
0.03
Mutation Rate
B
ITGAE
CDS1
C
CEP76
D
IKZF3
E

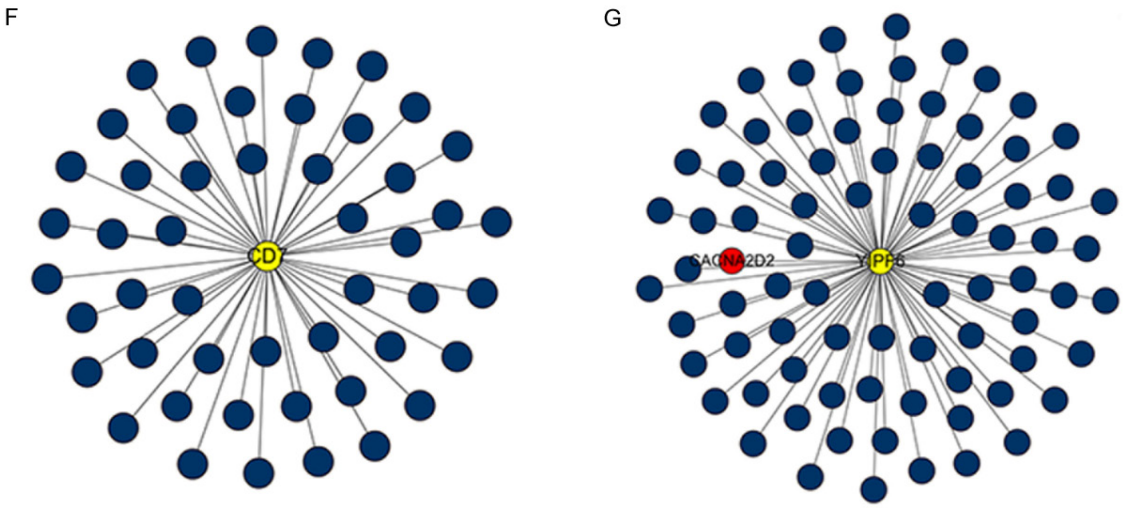

Figure 4. The statistical results of mutation frequencies of 24 mutated genes and relative function modules (the yellow is the driver gene, the blue is differential genes and the red is survival genes). A. The histogram of 24 mutation frequencies. B. KEGG function module driven by ITGAE; C. GO terms function module driven by CEP76; D. GO terms function module driven by IKZF3; E. GO terms function module driven by FGD6; F. GO terms function module driven by CD7; G. GO terms function module driven by YIPF6.

can be found in Table S4. Oxygenates may resist toxic substances (substances that are susceptible to cancer) of the invading cells [24] and partial nitrogen compounds inhibit certain processes in tumor cells [25].

(4) The mechanism of influence of the remaining terms.

The RHO proteins (Ras homolog gene family) act as molecular switches to control cellular processes, including cytoskeletal formation and cell migration [26]. Additionally, secreted substances affect the development of GBM to varying degrees. GBM migration is inhibited by both histone deacetylase SAHA and natural product andrographolide [27]. Furthermore, dexamethasone induces expression of neuronal and glial cell apoptosis markers [28]. During development, the diversity of forebrain complexity is also influenced by this signal path [29]. To sum up, all significantly enriched terms revealed crucial cancer mechanisms and these complex terms demonstrated the utility of integrated modules.

The "accelerated aging related mutation-differential expression" module revealed an important prognostic index

To investigate the relationship between the "accelerated aging related mutation-differential expression" modules and the clinical characteristics, a survival analysis was performed. As a result, 256 out of 11378 genes were identified to notable prognostic genes (Table S2). Some of the survival genes were integrated in modules (**Figure 4B** and **4C**), and details are shown in **Table 6**. Interestingly, MYOZ3 with the minimum *p*-value (about 0.001) has relevance to part of cell proliferation genes, hence it might be involved in regulating the aging and cancer growth progress [30]. Significant survival patterns were uncovered by the survival curves, even indicating that key survival genes were integrated in enriched modules (**Figure 6A-H**).

Discussion

The genomic dysfunction in molecular networks is the chief culprit that should be responsible for development of GBM, where aging acceleration is one of the driving incentives. The purposes of this study were as follows: (1) discriminating different age groups based on the normal brain of healthy people; (2) verifying the accelerated aging pattern of GBM compared by the normal group; (3) integrating accelerated aging related SNPs and differential expression thus exploring potential mechanisms of GBM based on aging acceleration.

In the immunosenescence theory of aging, a decline in functions in the immune system promote further dysfunctions in the neuroendocrine-immune axis as well as inflammation

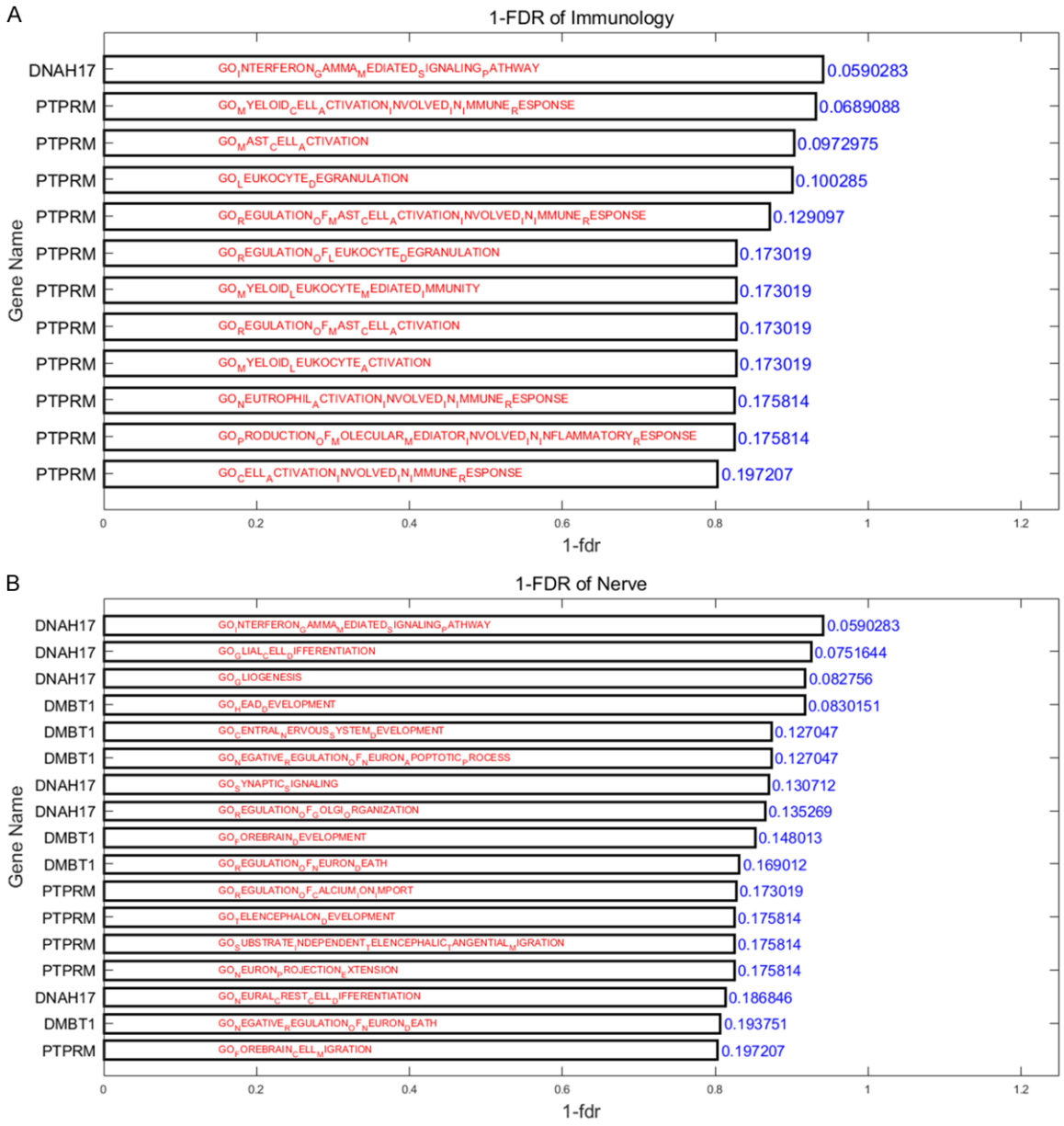

Figure 5. Enriched GO term results in the immune system and the nervous system. The left-most genes are mutated genes (driver genes), the medial contents are specific enriched GO terms, and the right-most values are the significance of GO terms in the module.

during the aging process [31]. In other words, accelerated aging is considered to lead to a disruption of the immune system, and dysregulation of the nervous system. As a result, cancer might be triggered. Our results further confirmed that TP53 and ABCB4 in mutated genes possessed the highest mutation rate and influence ratio, respectively. These results have been highly noted [5, 7]. In a prior study, the advanced aging process induced DNA damage, cell life reduction and apoptosis [32]; then cellular effects are caused by these changes in cellular and molecular levels irreversibly. The enriched GO functions in GBM modules coordinated with aging acceleration indicated that aging and GBM formation were affected by not only the nervous system, but also the endocrine and immunologic function [33]. In other words, all members of the intricate multifunctional system interact with others and then promote GBM progression together. Interestingly, significant GO terms showed that the occurrence of GBM was inseparable from the endocrine

Table 4. Enriched GO terms related to immunity

BP term	FDR
INTERFERON GAMMA MEDIATED SIGNALING PATHWAY	0.059
MYELOID CELL ACTIVATION INVOLVED IN IMMUNE RESPONSE	0.069
MAST CELL ACTIVATION	0.097
LEUKOCYTE DEGRANULATION	0.100
REGULATION OF MAST CELL ACTIVATION INVOLVED IN IMMUNE RESPONSE	0.129
MYELOID LEUKOCYTE ACTIVATION	0.173
REGULATION OF MAST CELL ACTIVATION	0.173
MYELOID LEUKOCYTE MEDIATED IMMUNITY	0.173
REGULATION OF LEUKOCYTE DEGRANULATION	0.173
PRODUCTION OF MOLECULAR MEDIATOR INVOLVED IN INFLAMMATORY RESPONSE	0.176
NEUTROPHIL ACTIVATION INVOLVED IN IMMUNE RESPONSE	0.176
CELL ACTIVATION INVOLVED IN IMMUNE RESPONSE	0.197

Table 5. Enriched GO terms related to nervous system

Biologic process	FDR
ASTROCYTE DIFFERENTIATION	0.050
GLIAL CELL DIFFERENTIATION	0.075
GLIOGENESIS	0.083
HEAD DEVELOPMENT	0.083
NEGATIVE REGULATION OF NEURON APOPTOTIC PROCESS	0.127
CENTRAL NERVOUS SYSTEM DEVELOPMENT	0.127
SYNAPTIC SIGNALING	0.131
REGULATION OF GOLGI ORGANIZATION	0.135
FOREBRAIN DEVELOPMENT	0.148
REGULATION OF NEURON DEATH	0.169
REGULATION OF CALCIUM ION IMPORT	0.173
NEURON PROJECTION EXTENSION	0.176
SUBSTRATE INDEPENDENT TELENCEPHALIC TANGENTIAL MIGRATION	0.176
TELENCEPHALON DEVELOPMENT	0.176
NEURAL CREST CELL DIFFERENTIATION	0.187
NEGATIVE REGULATION OF NEURON DEATH	0.194
FOREBRAIN CELL MIGRATION	0.197

Table 6. The survival genes with modules

Gene symbol					
ABLIM3	ADRB3	AFF3	ANGPTL2	BTN2A2	C14orf162
CACNA1G	CACNA2D2	CALCRL	CAMKV	CDK5RAP3	CDS1
CLIP3	CYB561	DCHS1	EPS8	GBP2	IQSEC2
KCNG1	MYLC2PL	NDUFA8	NHP2L1	NR1I2	PAK1IP1
PTPRT	RHBDL1	RPP25	SAT1	SLC22A1	SSBP3
TFF2	TOR3A	TUBD1	WASF1	WDR8	

regulation, the immunity system and the nervous system, thus indicating aging acceleration is one of the most important factors of GBM.

Integrating multi-omics profiles based on the proper network was informative to explore potential mechanisms of GBM, thus presenting a survival analysis [4, 34]. In addition, the aging acceleration was vital to promote the progression of cancers (also including GBM) [35]. Our results also indicated that the accelerated aging may be a risk index of GBM. In other words, molecular network modules in GBM provided a foundation for clinical therapeutics, and relative molecular markers (i.e. the immune system and the nervous system) were crucial to study the relationship between accelerated aging and GBM. Moreover, drug molecular treatment and targeted gene therapy came to insight of cancers. For instance, a signaling pathway suggested that dexamethasone can repress the development of the tumor [29].

Briefly, the tumor markers did not drive their functions alone, but interacted with each other within proper modules, then promoted development of GBM coordinately. In addition, GBM

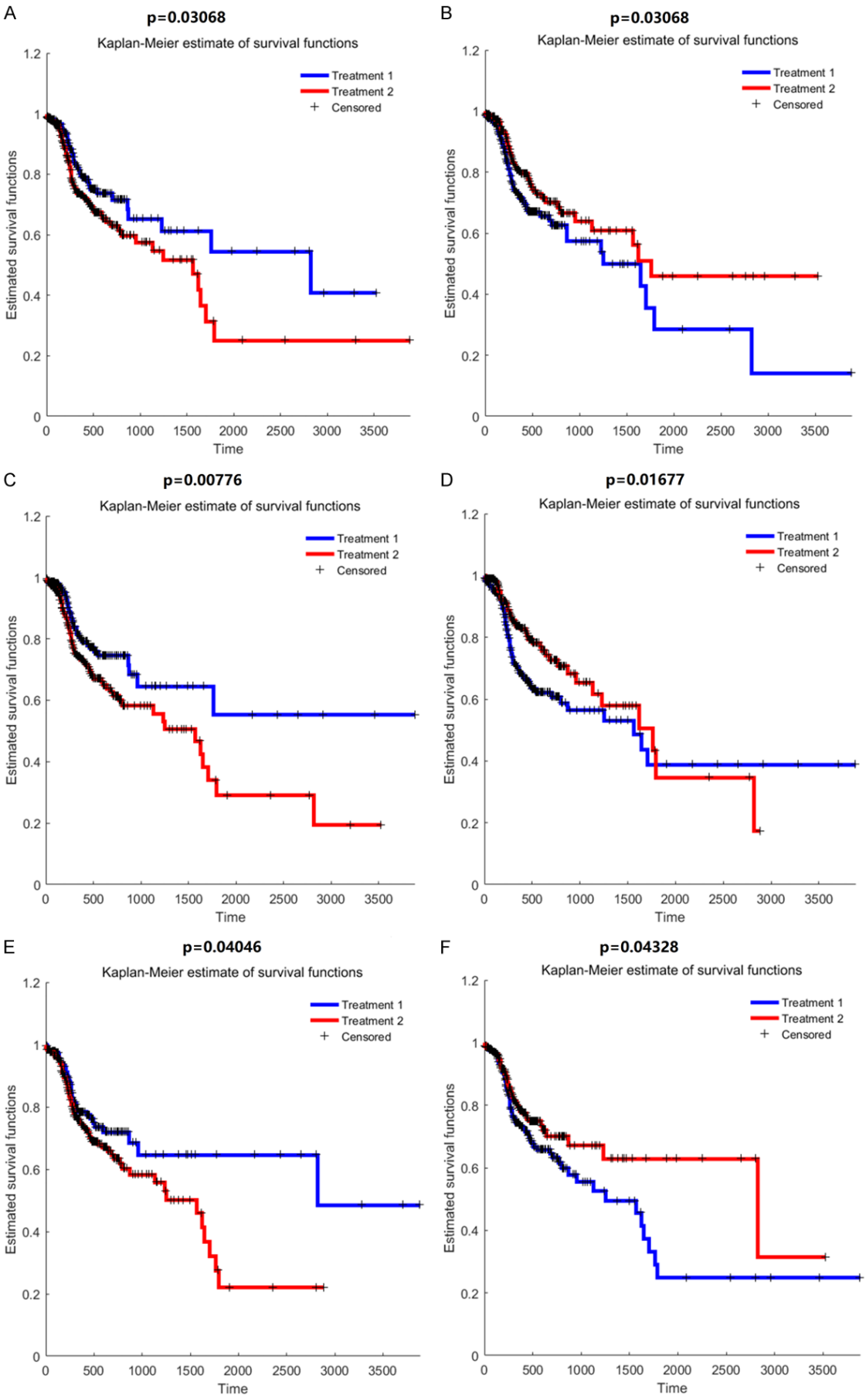
A
p=0.03068
Kaplan-Meier estimate of survival functions
Treatment 1
Treatment 2
Censored
Estimated survival functions
Time
B
p=0.03068
Kaplan-Meier estimate of survival functions
Treatment 1
Treatment 2
Censored
Estimated survival functions
Time
C
p=0.00776
Kaplan-Meier estimate of survival functions
Treatment 1
Treatment 2
Censored
Estimated survival functions
Time
D
p=0.01677
Kaplan-Meier estimate of survival functions
Treatment 1
Treatment 2
Censored
Estimated survival functions
Time
E
p=0.04046
Kaplan-Meier estimate of survival functions
Treatment 1
Treatment 2
Censored
Estimated survival functions
Time
F
p=0.04328
Kaplan-Meier estimate of survival functions
Treatment 1
Treatment 2
Censored
Estimated survival functions
Time

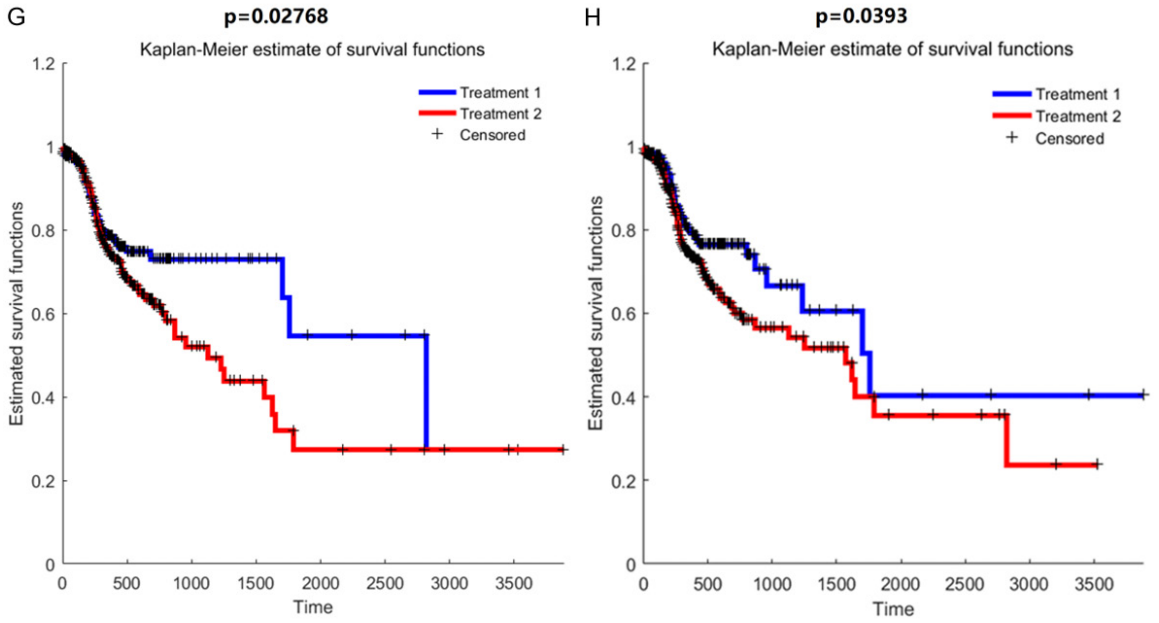

Figure 6. Survival curves of genes that were integrated in function modules. A. The survival curves of CDS1. B. The survival curves of BTN2A2. C. The survival curves of CAMKV. D. The survival curves of GBP2. E. The survival curves of RPP25. F. The survival curves of SAT1. G. The survival curves of SSBP3. H. The survival curves of CACNA2D2.

goes through a complicated process. Therefore, multi-scale analyses were apparently essential for GBM by focusing on potential biological functions. Our work identified important mechanisms (i.e. the immune system, the nervous system and the endocrine system) regulating GBM during the abnormal aging process coordinately. In summary, there are a series of dysfunctions promoting developments of GBM, in which aging acceleration was identified as a core factor in our work.

Acknowledgements

This work was supported by China Postdoctoral Science Foundation (2019M651175) and the National Key R&D Program of China (2016YFC0901704, 2017YFA0505500, 2017YFC0907505 and 2017YFC0908405). The funders had no role in study design, data collection and analysis, decision to publish, or preparation of the manuscript.

Disclosure of conflict of interest

None.

Address correspondence to: Yin Wang, Tumor Etiology and Screening Department of Cancer Institute and General Surgery, The First Affiliated Hospital of China Medical University, 155# North Nanjing Street, Heping District, Shenyang 110001, Liaoning Province, China. Tel: +86-13671726940; E-mail: chinawangyin@foxmail.com

References

[1] Kural KC, Tandon N, Skoblov M, Kel-Margoulis OV and Baranova AV. Pathways of aging: comparative analysis of gene signatures in replicative senescence and stress induced premature senescence. BMC Genomics 2016; 17 Suppl 14: 1030.

[2] Karczewski K and Snyder M. Integrative omics for health and disease. Nat Rev Genet 2018; 19: 299-310.

[3] Zhang X, Meng X, Chen Y, Sean XL and Haiyan Z. The biology of aging and cancer: frailty, inflammation, and immunity. Cancer J 2017; 23: 201-205.

[4] Dong H, Luo L, Hong S, Siu H, Xiao Y, Jin L, Chen R and Xiong M. Integrated analysis of mutations, miRNA and mRNA expression in glioblastoma. BMC Systems Biol 2010; 4: 163.

[5] Vauthier V, Ben Saad A, Elie J, Oumata N, Durand-Schneider AM, Bruneau A, Delaunay JL, Housset C, Aït-Slimane T, Meijer L and Falguières T. Structural analogues of roscovitine rescue the intracellular traffic and the function of ER-retained ABCB4 variants in cell models. Sci Rep 2019; 9: 6653.

[6] Wen C, Fu L, Huang J, Huang J, Dai Y, Wang B, Xu G, Wu L and Zhou H. Curcumin reverses doxorubicin resistance via inhibition the efflux

function of ABCB4 in doxorubicin-resistant breast cancer cells. Mol Med Rep 2019; 19: 5162-5168.
[7] Abdeen SK and Aqeilan RI. 2019: decoding the link between WWOX and p53 in aggressive breast cancer. Cell Cycle 2019; 10: 1-10.
[8] Demir S, Boldrin E, Sun Q, Hampp S, Tausch E, Eckert C, Eckert C, Ebinger M, Handgretinger R, Te Kronnie G, Wiesmuller L, Stilgenbauer S, Selivanova G, Debatin KM and Meyer LH. Therapeutic targeting of mutant p53 in pediatric acute lymphoblastic leukemia. Haematologica 2020; 105: 170-181.
[9] Mark C, David G, David D, Ruth C, Ken M and Patric T. Relevance of TP53 for CLL diagnostics. J Clin Pathol 2019; 72: 343-346.
[10] Li M, Hou T, Gao T, Lu X, Yang Q, Zhu Q, Li Z, Liu C, Mu G, Liu G, Bao Y, Wen H, Wang L, Wang H, Zhao Y, Gu W, Yang Y and Zhu WG. p53 cooperates with SIRT6 to regulate cardiolipin de novo biosynthesis. Cell Death Dis 2018; 9: 941.
[11] Dannhauser PN, Camus SM, Sakamoto K, Sadacca LA, Torres JA, Camus MD, Briant K, Vassilopoulos S, Rothnie A, Smith CJ and Brodsky FM. CHC22 and CHC17 clathrins have distinct biochemical properties and display differential regulation and function. J Biol Chem 2017; 292: 20834-20844.
[12] Nahorski MS, Borner GHH, Shaikh SS, Davies AK, Al-Gazali L, Antrobus R and Woods CG. Clathrin heavy chain 22 contributes to the control of neuropeptide degradation and secretion during neuronal development. Sci Rep 2018; 8: 2340.
[13] Schroder K, Hertzog PJ, Ravasi T and Hume DA. Interferon-gamma: an overview of signals, mechanisms and functions. J Leukoc Biol 2004; 75: 163-89.
[14] Chabot-Richards DS and George TI. Leukocytosis. Int J Lab Hematol 2014; 36: 279-88.
[15] Akin C. Mast cell activation syndromes. J Allergy Clin Immunol 2017; 140: 349-355.
[16] Minns D, Smith KJ and Findlay EG. Orchestration of adaptive T cell responses by neutrophil granule contents. Mediators Inflamm 2019; 2019: 8968943.
[17] Lucena-Cacace A, Umeda M, Navas LE and Carnero A. NAMPT as a dedifferentiation-inducer gene: NAD+ as core axis for glioma cancer stem-like cells maintenance. Front Oncol 2019; 9: 292.
[18] Konířová J, Oltová J, Corlett A, Kopycińska J, Kolář M, Bartůněk P and Zíková M. Modulated DISP3/PTCHD2 expression influences neural stem cell fate decisions. Sci Rep 2017; 7: 41597.
[19] Ando T, Kato R and Honda H. Identification of an early cell fate regulator by detecting dynamics in transcriptional heterogeneity and co-regulation during astrocyte differentiation. NPJ Syst Biol Appl 2019; 5: 18.
[20] Ohtaka-Maruyama C and Okado H. Molecular pathways underlying projection neuron production and migration during cerebral cortical development. Front Neurosci 2015; 9: 447.
[21] Marín O and Rubenstein JL. Cell migration in the forebrain. Annu Rev Neurosci 2003; 26: 441-83.
[22] Kempuraj D, Ahmed ME, Selvakumar GP, Thangavel R, Dhaliwal AS, Dubova I, Mentor S, Premkumar K, Saeed D, Zahoor H, Raikwar SP, Zaheer S, Iyer SS and Zaheer A. Brain injury-mediated neuroinflammatory response and Alzheimer's disease. Neuroscientist 2019; 16: 1073858419848293.
[23] Lavezzi AM, Ferrero S, Lattuada D, Piscioli F, Alfonsi G and Matturri L. 2018: pathobiological expression of the brain-derived neurotrophic factor (BDNF) in cerebellar cortex of sudden fetal and infant death victims. Int J Dev Neurosci 2018; 66: 9-17.
[24] Martins E, Silva V, Lemos A, Piscioli F, Alfonsi G and Matturri L. Newly synthesized oxygenated xanthones as potential p-glycoprotein activators: *in vitro, ex vivo*, and *in silico* studies. Molecules 2019; 24: 707.
[25] Liu JC, Narva S, Zhou K and Zhang W. A review on the antitumor activity of various nitrogenous-based heterocyclic compounds as NSCLC inhibitors. Mini Rev Med Chem 2019; 19: 1517-1530.
[26] Brandwein D and Wang Z. Interaction between Rho GTPases and 14-3-3 proteins. Int J Mol Sci 2017; 18: 2148.
[27] Chiu SP, Batsaikhan B, Huang HM and Wang JY. Application of electric cell-substrate impedance sensing to investigate the cytotoxic effects of andrographolide on U-87 MG glioblastoma cell migration and apoptosis. Sensors (Basel) 2019; 19: 2275.
[28] Lanshakov DA, Sukhareva EV, Kalinina TS and Dygalo NN. Dexamethasone-induced acute excitotoxic cell death in the developing brain. Neurobiol Dis 2016; 91: 1-9.
[29] Bielen H, Pal S, Tole S and Houart C. Temporal variations in early developmental decisions: an engine of forebrain evolution. Curr Opin Neurobiol 2017; 42: 152-159.
[30] Ye M, Ye F, He L and Houart C. Transcriptomic analysis of chicken Myozenin 3 regulation reveals its potential role in cell proliferation. PLoS One 2017; 12: e0189476.
[31] Fulop T, Larbi A, Dupuis G, Le Page A, Frost EH, Cohen AA, Witkowski JM and Franceschi C. Immunosenescence and inflamm-aging as two sides of the same coin: friends or foes? Front Immunol 2018; 8: 1960.

[32] Huang T, Zhang J, Xie L, Dong X, Zhang L, Cai Y and Li YX. Crosstissue coexpression network of aging. OMICS 2011; 15: 665.
[33] Arking R. Biology of aging: observations and principles. 3rd edition. New York: Oxford University Press; 2006.
[34] Mao YK, Liu ZB and Cai L. Identification of glioblastoma-specific prognostic biomarkers via an integrative analysis of DNA methylation and gene expression. Oncol Lett 2020; 20: 1619-1628.
[35] Horvath S. DNA methylation age of human tissues and cell types. Genome Biol 2013; 14: R115.

Table S1. Enriched modules with specific mutations and differential expression

	module2_kegg	module12_go	module15_go	module18_go	module19_go	module23_go
mutation gene	ITGAE	CEP76	IKZF3	FGD6	CD7	YIPF6
differential genes	ACCN1	ADAM23	AACS	ABCD4	AQP1	ABCD4
	ADRB1	APBB1	ABCG4	ABHD4	ARTN	AVPI1
	ALOX12B	BSCL2	ALDOC	ABHD8	ATP5C1	B4GALT6
	APBA2BP	C14orf147	ANK3	ACCN1	ATP6V0D1	BCHE
	ATP10D	C1orf121	ANKRD57	ACTR10	BAI2	BLM
	ATP2B3	C1orf27	AP2M1	AGTPBP1	BTG1	C12orf41
	ATP6V1A	C21orf62	BARD1	ANKMY2	CACNA1A	C16orf45
	AVPI1	C5orf3	BLM	AP2M1	CALM1	CACNA2D2
	BARD1	CBX3	BXDC5	ASCC3L1	CANX	CCT6A
	C10orf38	CCK	C21orf62	ATP13A2	CBX3	CHD5
	C10orf88	CNGA3	CD300A	ATP1A3	CDKL2	CHI3L1
	C17orf70	COL3A1	CHD5	ATP2B3	CENTB2	CORO1C
	C1orf121	CPLX2	CHGA	ATP6V1G2	CPSF4	CTNS
	C5orf3	CRH	CNNM2	ATP8A2	DCPS	CYBB
	CABP1	CRHBP	CPNE3	AYTL2	DOCK9	DENND2A
	CACNB1	DDX39	CSRP2	BAIAP2	F2R	ELAVL1
	CALD1	DOCK9	DDN	BASP1	FEZF2	ENPEP
	CDH9	EXTL1	DDX39	BLM	HLA-DPB1	FAAH
	CDKL2	F2R	DNM1	BTN2A2	INPP5F	FBXL2
	CDS1	FAM13A1	EHD3	C11orf49	KCNC1	FEM1C
	CHGA	FCER1G	FABP3	C11orf67	KDELR2	FGF13
	CLCN4	GNG13	FBXL2	C17orf70	LRP10	FREQ
	CMTM6	HHLA2	FCHO1	CACNB1	MDK	GABRA2
	COL4A2	HTR5A	FLJ20323	CACNB3	MLF2	GDF10
	COL5A2	IFI35	G3BP1	CAD	NAT11	GLS2
	CPEB1	IFRD1	GNB5	CAMK2A	NAV3	GNB5
	CRHBP	ING3	GREM2	CAMKV	NBL1	HIST1H1C
	CTNNA1	ITGAV	GUSB	CAMTA2	NDRG3	HLA-A
	CXCR4	KBTBD2	HNRPAB	CASP1	NECAP2	HLA-E
	CYP26B1	KCNV1	HS3ST2	CCT6A	NMNAT2	HOXB1
	DCPS	LAMB2	IDH1	CD93	NR4A2	ID3
	EFEMP1	LHX6	IFNGR2	CHD1	NY-REN-7	IRF2
	EHD4	LYN	IFRD1	CHGA	ODC1	JPH3
	ENPEP	MAST1	INTS12	CLCN4	OVOL2	KCTD5
	EPB49	NDEL1	KLHL26	CNGA3	PEPD	KIAA0284
	EPHB6	PADI1	LPPR2	CNOT2	PLEKHF2	KIAA1009
	FEM1C	PNMA2	NMI	COL4A2	POU3F2	LMO7
	G3BP1	PPP1R13B	NMNAT2	COX6C	PPL	LOC400451
	GAD2	RRP15	ODC1	CPEB1	PRKAB1	LPL
	GDF10	RUFY1	PAK3	CPLX3	PSMF1	LY6E
	GH2	RYR2	PAK6	CPT2	PTCH2	MADD
	GNB5	S100A4	PECI	CXCR4	PTPRZ1	MAN2B1
	HCN2	SLIT3	PHYHIP	DAG1	SLC6A13	MAPK8IP2
	HEATR2	SNCG	PLAT	DCPS	STAR	MATN2
	HIST1H1C	SPDEF	PLOD3	DDX23	SYNJ2	NMNAT2
	HLA-F	SYN2	PYGL	DKFZP56400823	TMCO1	NOLC1
	HNRPK	TAGLN	RAP1A	DNAJC12	TMEM24	NRXN3

HPRT1
HRH3
IFI16
IGFBP2
IKBKB
INPP5F
KCNJ3
KCNV1
KDELR2
KHDRBS2
KIAA0143
LDB3
LIMA1
LMO7
MARK4
MTX2
NBL1
NES
NPAL3
OCA2
P2RX5
PAK3
PALLD
PCSK2
PDE2A
PDE4DIP
PDIA4
PDK2
PHC2
PHYHIP
PLOD3
PPP1R13B
PSMF1
PUS7
RAB11FIP2
RFXANK
RIMS3
RNF208
RPLP2
RYR2
SCAMP2
SCN8A
SH3GLB2
SHANK2
SNRPF
SOX9
STS
STXBP6
SULT4A1
SYNCRIP
TLR2
TPPP
VAMP2
VEZF1
WNT10B
RND2
S100A4
SERPINA1
SERPINH1
SNAP25
SNCA
SNRPF
SPTBN2
SULT4A1
SYT1
TAGLN
TERF2IP
TNNT1
TOR1AIP1
TREM2
TYRO3
VSNL1
ZDHHC4
DRD1
DYNC1I1
EFCBP2
EHD3
FGF13
FHOD3
FKBP10
FLT3
FSTL4
FTSJ2
GABRA4
GALNT1
GARNL4
GBP1
GBP2
GNG13
GRIN2A
GRM7
HAGH
HCLS1
HES1
HLA-C
HLA-DPB1
HLA-F
ICAM5
IFI16
IFI30
INA
ITFG1
ITGB2
JMJD1B
KCNN1
KIAA0355
KIAA0774
KIAA1467
LAMB2
LAP3
LIG4
LOC400451
LRP10
MAP1S
MAPK1
MAPK3
MATN2
MCF2
MCM7
MDM1
MGLL
MGST2
MYO9B
VEZF1
ZMPSTE24
ODC1
OSBP2
PGLS
PHYHIP
POLD2
PTPRZ1
QTRT1
RAB3B
RASAL1
RBBP4
RGS1
RND2
SCAMP4
SEMA4A
SHANK2
SHMT2
SLC16A1
SLC2A10
SLC30A3
SLITRK5
SNRPF
SOSTDC1
STAT4
TMEM24
TNC
TYRO3
ULK1
VGLL4
VIPR1
VPS53
XK
ZNF140
ZNF45

SYNJ1
TIMELESS
TP53
TSPYL2
TXNDC1
USP8

NAV3
NECAP1
NEFM
NMNAT2
NOL5A
NOL8
NOX4
NPAL3
NTSR1
NUP133
NXT2
OXR1
PADI3
PAK3
PALLD
PDCL3
PDE1A
PDE1B
PDE2A
PDE4A
PFKM
PFKP
PHACTR1
PHACTR4
PIP5K1C
PLSCR1
POU3F2
PPM2C
PRB3
PRKAR1B
PRMT8
PRPF4B
PRR14
PSMF1
PYGL
RAB8A
RAB9A
RAP2B
RBM7
RBP4
RIMBP2
RIMS2
RPP25
RRAGC
RUSC2
S100A4
SAP30BP
SAT1
SBF1
SCN2B

SEMA6B
SERINC3
SERPINH1
SH3BP5
SH3GL2
SLIT3
SMAD1
SMARCC1
SMARCE1
SMPX
SORBS2
SOX2
SOX9
SSBP3
SSR1
STAG2
STS
SYT13
TDG
TLR2
TM9SF1
TNC
TUBA4A
TXNDC1
XK
YWHAB
ZCCHC8
ZFAND3
ZMPSTE24
ZNF20
ZNF200
ZNF302

Table S2. 256 survival genes

survival genes
C20orf19
MAGEA10
CRLF1
LPIN2
BAAT
THBS2
BTN2A2
CLEC1B
EMP3
NFYB
ASPSCR1
GGTLA4
MGMT
SDC4

KIF18A
TMEM48
PROL1
SLC26A1
SLC30A10
TNFRSF1B
SIT1
CLIP3
CDC14B
LEP
ZNF85
APOOL
RPP25
PHEX
TNFRSF4
GNL3
C14orf162
ZAP70
DDX3X
NAT8B
NUP155
GMPR
ZNF606
NPY5R
LY9
ATXN7
HLF
SOCS1
AMOTL2
MEIS1
NDUFA8
FBXO7
HIP1R
GBP2
HIST3H2A
MRPL49
NME6
PDE6B
TUBD1
EPS8
SLC22A6
OR5I1
NLRP3
SLC22A1
AFF3
GUCY2F
TMOD2
GGCX
C20orf32
C10orf92

TNFRSF13B
GUCY2C
CACNA1F
NR2F2
AKAP3
BDKRB1
PCDHB12
ASCL3
SPSB1
NDUFAB1
ZSCAN16
XPO1
C8G
IQSEC2
RPGR
UMOD
CYB561
RBKS
SRPR
CLTCL1
NCAM2
NSFL1C
GALK2
HIF3A
PTPN21
SPTB
AFG3L2
LAMB1
HOXC8
PQBP1
WDR8
MLC1
TLK2
STK10
KIAA0196
PAK1IP1
SMUG1
VGLL1
TREX2
KRT13
F2RL3
ACADL
IL23A
FRAT2
VAPB
CTSG
SLC6A5
ACE
ONECUT1

OR3A3
TAF10
MYL2
SIPA1L1
PTPRT
ADRB3
MYCT1
PLAC8
CACNA2D2
ACTL7B
KCNA10
PNMT
ZNF8
STARD3
ABLIM3
MRPL41
CFP
AHR
E2F1
NPVF
SCARB1
CLDN1
ZNF287
GDPD5
IL13RA2
HOMER2
EPHB4
RAC2
RGS13
GRAP2
CPN1
OMP
RFC5
ABCC10
A4GNT
SMARCA1
RAB30
CDK7
FAM125B
IL20RA
TOR3A
CDC2L6
CCL4
TGM2
CAPN9
IL5RA
SLC38A4
KCNG1
PASK
AQP4

MTL5
NFATC1
CDK5RAP3
TREML2
UNC119
HYAL4
RAP2A
CALCRL
SH2D1A
JUNB
DPP3
CACNA1G
CPE
KIAA0391
ABCA6
CPB2
GFI1
VPS26A
FOSL2
GRIA4
MMP2
C11orf71
MYOZ3
CCNT1
CFTR
CHMP6
TNFSF8
GLRA1
DCHS1
SLC4A5
MYLC2PL
OR10C1
SLC15A3
TPBG
FOXL1
RASL11B
NR1I2
FGD2
GFPT2
WASF1
NHP2L1
GGTLA1
MCCC1
NAV2
STK16
PMAIP1
PYGM
LRPPRC
ELA3A

TSEN2
LILRA3
SLC29A2
LCT
CNDP2
RHBDL1
DHX9
AFAP1
PAFAH1B2
AHDC1
C2orf47
HGD
CAMKV
CETN2
C1QTNF3
FLJ21986
TAS2R7
C1QL1
LIPF
LRRC42
OR10J1
FAM50B
C18orf25
NDST2
TTC12
PRG2
ZDHHC13
OGG1
SAT1
ALX3
PHTF1
ANGPTL2
SSBP3
DSCR6
TFF2
CDS1
METAP1
MAGEB3
SYCP1
ERBB2
VSX1
WRB
BMP2
RFX2

Table S3. Enriched GO terms (a total of 57 terms)

GO_terms	modules	FDR	function	link
3796	15	0.001827	GO_CLATHRIN_MEDIATED_ENDOCYTOSIS	http://www.broadinstitute.org/gsea/msigdb/cards/GO_CLATHRIN_MEDIATED_ENDOCYTOSIS
1926	23	0.00576	GO_LEARNING	http://www.broadinstitute.org/gsea/msigdb/cards/GO_LEARNING
2202	18	0.049685	GO_ASTROCYTE_DIFFERENTIATION	http://www.broadinstitute.org/gsea/msigdb/cards/GO_ASTROCYTE_DIFFERENTIATION
2560	18	0.059028	GO_INTERFERON_GAMMA_MEDIATED_SIGNALING_PATHWAY	http://www.broadinstitute.org/gsea/msigdb/cards/GO_INTERFERON_GAMMA_MEDIATED_SIGNALING_PATHWAY
3236	12	0.068909	GO_MYELOID_CELL_ACTIVATION_INVOLVED_IN_IMMUNE_RESPONSE	http://www.broadinstitute.org/gsea/msigdb/cards/GO_MYELOID_CELL_ACTIVATION_INVOLVED_IN_IMMUNE_RESPONSE
1056	18	0.069615	GO_RESPONSE_TO_EPIDERMAL_GROWTH_FACTOR	http://www.broadinstitute.org/gsea/msigdb/cards/GO_RESPONSE_TO_EPIDERMAL_GROWTH_FACTOR
105	18	0.075164	GO_RESPONSE_TO_NITROGEN_COMPOUND	http://www.broadinstitute.org/gsea/msigdb/cards/GO_RESPONSE_TO_NITROGEN_COMPOUND
3421	18	0.075164	GO_GLIAL_CELL_DIFFERENTIATION	http://www.broadinstitute.org/gsea/msigdb/cards/GO_GLIAL_CELL_DIFFERENTIATION
1753	18	0.082756	GO_GLIOGENESIS	http://www.broadinstitute.org/gsea/msigdb/cards/GO_GLIOGENESIS
2732	19	0.083015	GO_HEAD_DEVELOPMENT	http://www.broadinstitute.org/gsea/msigdb/cards/GO_HEAD_DEVELOPMENT
1670	12	0.089297	GO_REGULATION_OF_SECRETION	http://www.broadinstitute.org/gsea/msigdb/cards/GO_REGULATION_OF_SECRETION
1441	12	0.097298	GO_MAST_CELL_ACTIVATION	http://www.broadinstitute.org/gsea/msigdb/cards/GO_MAST_CELL_ACTIVATION
2449	12	0.097298	GO_POSITIVE_REGULATION_OF_CELL_DEATH	http://www.broadinstitute.org/gsea/msigdb/cards/GO_POSITIVE_REGULATION_OF_CELL_DEATH
259	12	0.100285	GO_LEUKOCYTE_DEGRANULATION	http://www.broadinstitute.org/gsea/msigdb/cards/GO_LEUKOCYTE_DEGRANULATION
1931	12	0.100285	GO_REGULATION_OF_CELLULAR_LOCALIZATION	http://www.broadinstitute.org/gsea/msigdb/cards/GO_REGULATION_OF_CELLULAR_LOCALIZATION
3586	12	0.100285	GO_REGULATION_OF_TRANSPORT	http://www.broadinstitute.org/gsea/msigdb/cards/GO_REGULATION_OF_TRANSPORT
115	19	0.127047	GO_NEGATIVE_REGULATION_OF_NEURON_APOPTOTIC_PROCESS	http://www.broadinstitute.org/gsea/msigdb/cards/GO_NEGATIVE_REGULATION_OF_NEURON_APOPTOTIC_PROCESS
2986	19	0.127047	GO_CELLULAR_RESPONSE_TO_KETONE	http://www.broadinstitute.org/gsea/msigdb/cards/GO_CELLULAR_RESPONSE_TO_KETONE
3949	19	0.127047	GO_CELLULAR_RESPONSE_TO_DEXAMETHASONE_STIMULUS	http://www.broadinstitute.org/gsea/msigdb/cards/GO_CELLULAR_RESPONSE_TO_DEXAMETHASONE_STIMULUS
4048	19	0.127047	GO_CENTRAL_NERVOUS_SYSTEM_DEVELOPMENT	http://www.broadinstitute.org/gsea/msigdb/cards/GO_CENTRAL_NERVOUS_SYSTEM_DEVELOPMENT
377	12	0.129097	GO_SECRETION_BY_CELL	http://www.broadinstitute.org/gsea/msigdb/cards/GO_SECRETION_BY_CELL
546	12	0.129097	GO_REGULATION_OF_MAST_CELL_ACTIVATION_INVOLVED_IN_IMMUNE_RESPONSE	http://www.broadinstitute.org/gsea/msigdb/cards/GO_REGULATION_OF_MAST_CELL_ACTIVATION_INVOLVED_IN_IMMUNE_RESPONSE
3719	12	0.129097	GO_REGULATION_OF_ION_TRANSPORT	http://www.broadinstitute.org/gsea/msigdb/cards/GO_REGULATION_OF_ION_TRANSPORT
4369	12	0.129097	GO_CELLULAR_RESPONSE_TO_ALKALOID	http://www.broadinstitute.org/gsea/msigdb/cards/GO_CELLULAR_RESPONSE_TO_ALKALOID
704	18	0.130712	GO_LUNG_MORPHOGENESIS	http://www.broadinstitute.org/gsea/msigdb/cards/GO_LUNG_MORPHOGENESIS
2579	18	0.130712	GO_SYNAPTIC_SIGNALING	http://www.broadinstitute.org/gsea/msigdb/cards/GO_SYNAPTIC_SIGNALING
39	18	0.135269	GO_REGULATION_OF_GOLGI_ORGANIZATION	http://www.broadinstitute.org/gsea/msigdb/cards/GO_REGULATION_OF_GOLGI_ORGANIZATION
1808	18	0.135269	GO_CELLULAR_RESPONSE_TO_ORGANIC_SUBSTANCE	http://www.broadinstitute.org/gsea/msigdb/cards/GO_CELLULAR_RESPONSE_TO_ORGANIC_SUBSTANCE
2482	18	0.136146	GO_CELLULAR_RESPONSE_TO_NITROGEN_COMPOUND	http://www.broadinstitute.org/gsea/msigdb/cards/GO_CELLULAR_RESPONSE_TO_NITROGEN_COMPOUND
1120	19	0.148013	GO_FOREBRAIN_DEVELOPMENT	http://www.broadinstitute.org/gsea/msigdb/cards/GO_FOREBRAIN_DEVELOPMENT
3288	19	0.153433	GO_RESPONSE_TO_DEXAMETHASONE	http://www.broadinstitute.org/gsea/msigdb/cards/GO_RESPONSE_TO_DEXAMETHASONE
3134	19	0.169012	GO_REGULATION_OF_NEURON_DEATH	http://www.broadinstitute.org/gsea/msigdb/cards/GO_REGULATION_OF_NEURON_DEATH
1740	12	0.173019	GO_MYELOID_LEUKOCYTE_ACTIVATION	http://www.broadinstitute.org/gsea/msigdb/cards/GO_MYELOID_LEUKOCYTE_ACTIVATION
1876	12	0.173019	GO_REGULATION_OF_CALCIUM_ION_IMPORT	http://www.broadinstitute.org/gsea/msigdb/cards/GO_REGULATION_OF_CALCIUM_ION_IMPORT
1977	12	0.173019	GO_REGULATION_OF_MAST_CELL_ACTIVATION	http://www.broadinstitute.org/gsea/msigdb/cards/GO_REGULATION_OF_MAST_CELL_ACTIVATION

2482	12	0.173019	GO_CELLULAR_RESPONSE_TO_NITROGEN_COMPOUND	http://www.broadinstitute.org/gsea/msigdb/cards/GO_CELLULAR_RESPONSE_TO_NITROGEN_COMPOUND
2693	12	0.173019	GO_MYELOID_LEUKOCYTE_MEDIATED_IMMUNITY	http://www.broadinstitute.org/gsea/msigdb/cards/GO_MYELOID_LEUKOCYTE_MEDIATED_IMMUNITY
3553	12	0.173019	GO_REGULATION_OF_LEUKOCYTE_DEGRANULATION	http://www.broadinstitute.org/gsea/msigdb/cards/GO_REGULATION_OF_LEUKOCYTE_DEGRANULATION
292	12	0.175814	GO_NEURON_PROJECTION_EXTENSION	http://www.broadinstitute.org/gsea/msigdb/cards/GO_NEURON_PROJECTION_EXTENSION
645	12	0.175814	GO_POSITIVE_REGULATION_OF_RHO_PROTEIN_SIGNAL_TRANSDUCTION	http://www.broadinstitute.org/gsea/msigdb/cards/GO_POSITIVE_REGULATION_OF_RHO_PROTEIN_SIGNAL_TRANSDUCTION
990	12	0.175814	GO_CELLULAR_RESPONSE_TO_OXYGEN_CONTAINING_COMPOUND	http://www.broadinstitute.org/gsea/msigdb/cards/GO_CELLULAR_RESPONSE_TO_OXYGEN_CONTAINING_COMPOUND
1281	12	0.175814	GO_SECRETION	http://www.broadinstitute.org/gsea/msigdb/cards/GO_SECRETION
1634	12	0.175814	GO_CELLULAR_RESPONSE_TO_HORMONE_STIMULUS	http://www.broadinstitute.org/gsea/msigdb/cards/GO_CELLULAR_RESPONSE_TO_HORMONE_STIMULUS
1642	12	0.175814	GO_SUBSTRATE_INDEPENDENT_TELENCEPHALIC_TANGENTIAL_MIGRATION	http://www.broadinstitute.org/gsea/msigdb/cards/GO_SUBSTRATE_INDEPENDENT_TELENCEPHALIC_TANGENTIAL_MIGRATION
1822	12	0.175814	GO_REGULATION_OF_ENDOCRINE_PROCESS	http://www.broadinstitute.org/gsea/msigdb/cards/GO_REGULATION_OF_ENDOCRINE_PROCESS
1937	12	0.175814	GO_PRODUCTION_OF_MOLECULAR_MEDIATOR_INVOLVED_IN_INFLAMMATORY_RESPONSE	http://www.broadinstitute.org/gsea/msigdb/cards/GO_PRODUCTION_OF_MOLECULAR_MEDIATOR_INVOLVED_IN_INFLAMMATORY_RESPONSE
2264	12	0.175814	GO_RESPONSE_TO_OXYGEN_CONTAINING_COMPOUND	http://www.broadinstitute.org/gsea/msigdb/cards/GO_RESPONSE_TO_OXYGEN_CONTAINING_COMPOUND
3640	12	0.175814	GO_NEUTROPHIL_ACTIVATION_INVOLVED_IN_IMMUNE_RESPONSE	http://www.broadinstitute.org/gsea/msigdb/cards/GO_NEUTROPHIL_ACTIVATION_INVOLVED_IN_IMMUNE_RESPONSE
3792	12	0.175814	GO_TELENCEPHALON_DEVELOPMENT	http://www.broadinstitute.org/gsea/msigdb/cards/GO_TELENCEPHALON_DEVELOPMENT
4091	12	0.175814	GO_REGULATED_EXOCYTOSIS	http://www.broadinstitute.org/gsea/msigdb/cards/GO_REGULATED_EXOCYTOSIS
4320	12	0.175814	GO_REGULATION_OF_TRANSMEMBRANE_TRANSPORT	http://www.broadinstitute.org/gsea/msigdb/cards/GO_REGULATION_OF_TRANSMEMBRANE_TRANSPORT
3209	12	0.184613	GO_CELLULAR_RESPONSE_TO_ENDOGENOUS_STIMULUS	http://www.broadinstitute.org/gsea/msigdb/cards/GO_CELLULAR_RESPONSE_TO_ENDOGENOUS_STIMULUS
4207	18	0.186846	GO_NEURAL_CREST_CELL_DIFFERENTIATION	http://www.broadinstitute.org/gsea/msigdb/cards/GO_NEURAL_CREST_CELL_DIFFERENTIATION
3993	19	0.193751	GO_NEGATIVE_REGULATION_OF_NEURON_DEATH	http://www.broadinstitute.org/gsea/msigdb/cards/GO_NEGATIVE_REGULATION_OF_NEURON_DEATH
516	12	0.197207	GO_RESPONSE_TO_WOUNDING	http://www.broadinstitute.org/gsea/msigdb/cards/GO_RESPONSE_TO_WOUNDING
1239	12	0.197207	GO_FOREBRAIN_CELL_MIGRATION	http://www.broadinstitute.org/gsea/msigdb/cards/GO_FOREBRAIN_CELL_MIGRATION
1285	12	0.197207	GO_CELL_ACTIVATION_INVOLVED_IN_IMMUNE_RESPONSE	http://www.broadinstitute.org/gsea/msigdb/cards/GO_CELL_ACTIVATION_INVOLVED_IN_IMMUNE_RESPONSE

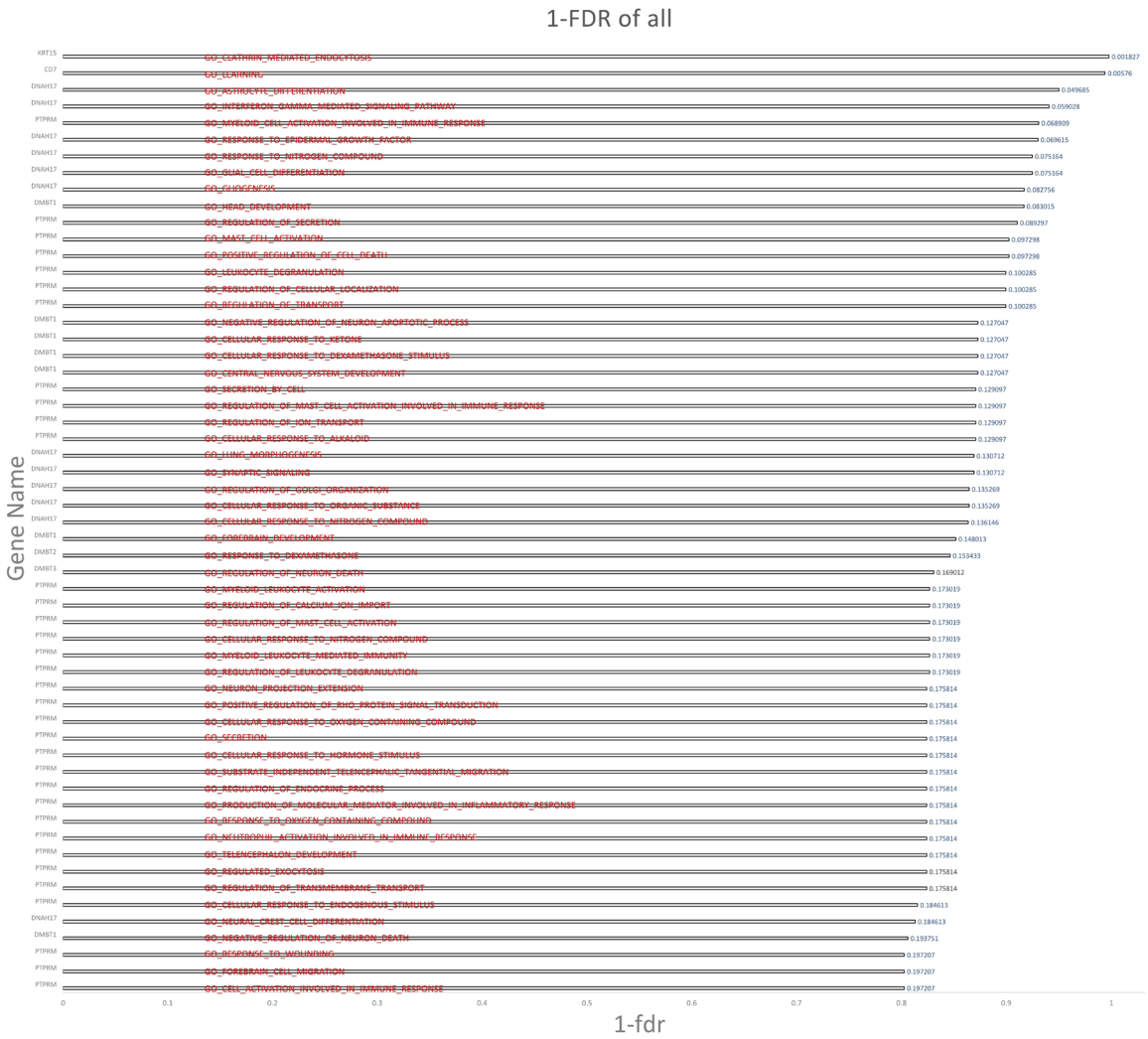

Figure S1. All enriched GO functions and significances.

Table S4. Enriched GO terms regarding the influences of stimuli and compounds

function	link	module	FDR
GO_RESPONSE_TO_EPIDERMAL_GROWTH_FACTOR	http://www.broadinstitute.org/gsea/msigdb/cards/GO_RESPONSE_TO_EPIDERMAL_GROWTH_FACTOR	18	0.069615
GO_RESPONSE_TO_NITROGEN_COMPOUND	http://www.broadinstitute.org/gsea/msigdb/cards/GO_RESPONSE_TO_NITROGEN_COMPOUND	18	0.075164
GO_CELLULAR_RESPONSE_TO_KETONE	http://www.broadinstitute.org/gsea/msigdb/cards/GO_CELLULAR_RESPONSE_TO_KETONE	19	0.127047
GO_CELLULAR_RESPONSE_TO_DEXAMETHASONE_STIMULUS	http://www.broadinstitute.org/gsea/msigdb/cards/GO_CELLULAR_RESPONSE_TO_DEXAMETHASONE_STIMULUS	19	0.127047
GO_CELLULAR_RESPONSE_TO_ALKALOID	http://www.broadinstitute.org/gsea/msigdb/cards/GO_CELLULAR_RESPONSE_TO_ALKALOID	12	0.129097
GO_CELLULAR_RESPONSE_TO_ORGANIC_SUBSTANCE	http://www.broadinstitute.org/gsea/msigdb/cards/GO_CELLULAR_RESPONSE_TO_ORGANIC_SUBSTANCE	18	0.135269
GO_CELLULAR_RESPONSE_TO_NITROGEN_COMPOUND	http://www.broadinstitute.org/gsea/msigdb/cards/GO_CELLULAR_RESPONSE_TO_NITROGEN_COMPOUND	18	0.136146
GO_RESPONSE_TO_DEXAMETHASONE	http://www.broadinstitute.org/gsea/msigdb/cards/GO_RESPONSE_TO_DEXAMETHASONE	19	0.153433
GO_CELLULAR_RESPONSE_TO_NITROGEN_COMPOUND	http://www.broadinstitute.org/gsea/msigdb/cards/GO_CELLULAR_RESPONSE_TO_NITROGEN_COMPOUND	12	0.173019
GO_CELLULAR_RESPONSE_TO_OXYGEN_CONTAINING_COMPOUND	http://www.broadinstitute.org/gsea/msigdb/cards/GO_CELLULAR_RESPONSE_TO_OXYGEN_CONTAINING_COMPOUND	12	0.175814
GO_CELLULAR_RESPONSE_TO_ENDOGENOUS_STIMULUS	http://www.broadinstitute.org/gsea/msigdb/cards/GO_CELLULAR_RESPONSE_TO_ENDOGENOUS_STIMULUS	12	0.184613